

Protein expression profiles following
radiation in a rat cirrhotic model

Sook In Chung

Department of Medical Science
The Graduate School, Yonsei University

Protein expression profiles following radiation in a rat cirrhotic model

Directed by Professor Kwang-Hyub Han

The Master's Thesis
submitted to the Department of Medical Science
the Graduate School of Yonsei University
in partial fulfillment of the requirements for the
degree of Master of Medical Science

Sook In Chung

December 2007

This certifies that the masters thesis of
Chung, Sook-In is approved.

Thesis Supervisor :

Thesis Committee Member #1 :

Thesis Committee Member #2 :

Department of Medical Science

The Graduate School
Yonsei University

December 2007

TABLE OF CONTENTS

ABSTRACT	1
I. INTRODUCTION	4
II. MATERIALS AND METHODS	7
1. Animals	7
2. Induction of liver cirrhosis	7
3. Experimental groups	8
4. Histologic analysis	8
A. Picro-Sirius red stain	
B. Immunohistochemical stain	
5. Biochemical parameters	10
6. Proteomic analysis	10
A. Two Dimensional Electrophoresis	
B. In gel digestion	
C. Quadrupole time of flight (Q-TOF) and data processing	
7. Western blot analysis	13
8. Statistical analysis	14
III. RESULTS	15
1. The optical examination of TAA-induced liver cirrhosis in rats	15

2. Measurement of liver weight	16
3. Histological assay and measurement of fibrotic area	17
4. Assessment of biochemical parameters in experimental groups	20
5. Proteomic analysis and validation	21
6. Immunohistochemical staining for PCNA and hematoxylin- eosin staining	25
IV. DISCUSSION	28
V. CONCLUSION	31
REFERENCES	32
ABSTRACT (IN KOREAN)	38

LIST OF FIGURES

Figure 1. Gross photographs of rat liver	15
Figure 2. Histological analysis by Masson's trichrome and picro-sirius red staining	18
Figure 3. Quantitative analysis of liver fibrosis	19
Figure 4. Differential expression of proteins	22
Figure 5. Validation of common proteins	24
Figure 6. Immunohistochemical staining for PCNA	26
Figure 7. Hematoxylin and eosin staining of liver sections	26
Figure 8. Quantitative analysis of immunohistochemical staining for PCNA (A) and hematoxylin and eosin staining	27

LIST OF TABLES

Table 1. Comparison of liver/body weight ratio between TAA-alone group and TAA-plus-radiation group ·	16
Table 2. Biological parameters in serum by intraperitoneal administration of TAA · · · · ·	20
Table 3. Proteins that were altered by radiation · · · · ·	23

ABSTRACT

Protein expression profiles following
radiation in a rat cirrhotic model

Sook In Chung

*Department of Medical Science
The Graduate School, Yonsei University*

(Directed by Professor Kwang-Hyub Han)

Hepatocellular carcinoma (HCC) is one of the most common malignancies in Asia as well as worldwide. It has a poor prognosis due to its rapid progression and the complicating liver cirrhosis. Radiation therapy (RT) is one of several treatments for HCC. It has been tried to HCC in mild-to-moderate degree of associated liver cirrhosis. However, information is insufficient on the tolerance of RT in liver cirrhosis. The

aim of this study is to assess radiation effect on cirrhotic liver and to identify common proteins in liver tissue and serum following radiation exposure in rats with thioacetamide (TAA)-induced liver cirrhosis.

Male Wistar rats were treated with 0.3 g/L TAA in their drinking water for 9 weeks. To determine if radiation was associated with hepatic injury, two experimental groups were examined: TAA-alone and TAA-plus-radiation, with three rats in each group. The livers of the cirrhotic rats were subjected to 10 Gy radiation and the animals were killed 3 weeks later. The development of liver cirrhosis was observed histologically. Proteins from liver tissue and serum were analyzed using two-dimensional electrophoresis and identified using quadrupole time of flight (Q-TOF) mass spectrometry (MS). Identified proteins were validated using Western blotting.

Histological examination showed that hepatic fibrosis more increased following radiation in TAA-induced liver cirrhosis. In the proteomic analysis of liver tissue and serum, 57 proteins differed significantly between the TAA-alone and TAA-plus-radiation groups. The identified proteins had functions in the immune response, signal transduction, apoptosis, proliferation/differentiation, and reactive oxygen species metabolism. Common proteins in liver tissue and serum following radiation were the heparanase precursor and the hepatocyte growth factor receptor. Expression of the heparanase precursor increased twofold in the TAA-plus-radiation group compared to the TAA-alone group, while the expression of the hepatocyte growth factor receptor decreased twofold in the TAA-plus-radiation group. The expression of proliferating cell nuclear

antigen (PCNA) decreased following radiation, just like the hepatocyte growth factor receptor. However, hematoxylin and eosin staining showed that apoptotic cells increased following radiation.

In conclusion, radiation induced hepatic fibrosis and apoptosis in TAA-induced liver cirrhosis. The heparanase precursor increased and hepatocyte growth factor receptor decreased both in liver tissue and serum, suggesting that these proteins may be useful in detecting and monitoring radiation-induced hepatic injury.

Key words : liver cirrhosis, radiation, proteomics, hepatic injury

Protein expression profiles following
radiation in a rat cirrhotic model

Sook In Chung

*Department of Medical Science
The Graduate School, Yonsei University*

(Directed by Professor Kwang-Hyub Han)

I. INTRODUCTION

Hepatocellular carcinoma (HCC) is one of the most common malignancies worldwide, especially in Asia.¹⁻⁴ It has a poor prognosis because of its rapid progression and the complicating liver cirrhosis.⁵ Although the most effective treatment is surgical resection, such

procedure is still limited even for small tumors.⁶⁻⁸ Furthermore, resection is impossible at diagnosis in more than 80% patients because of the advanced stage of the disease at the time of clinical presentation or poor hepatic functional reserve associated with liver cirrhosis.^{1,4}

For the majority of patients with HCC who are technically unresectable or medically inoperable, various treatments have been used, which include transcatheter arterial chemoembolization (TACE), percutaneous ethanol injection therapy, microwave coagulation therapy, and liver transplantation.^{2,4,9-11} However, none of these nonsurgical modalities has been very successful.¹²

Radiation therapy (RT) has been tried for HCC since the 1970s.¹³ Although RT is one of the most effective modalities for treating malignant neoplasms in general, RT has rarely been used to treat HCC. A major reason for this limited use is the low radiation tolerance of the whole liver, as low as 35 Gy, which is typically lower than the therapeutic dose needed for tumor control.^{8,12,14}

However, some reports suggest that the tolerable dose for the liver also depends on the irradiated liver volume, indicating that a small volume of liver can tolerate a high dose without causing serious hepatic problems. Consequently, the application of RT in management of hepatic tumors has been increasingly recognized.¹⁵

Unfortunately, the frequent association of concurrent liver disease, such as liver cirrhosis, poses a major challenge in pursuing the therapeutic goal of tumor control with minimum toxicity.¹⁶⁻¹⁸ However, with a mild-to-moderate degree of associated liver cirrhosis, radiotherapy can still be applied to the treatment of HCC.^{1,15}

In a previous study, a thioacetamide (TAA)-induced rat liver cirrhosis

model showed expression of a repertoire of proteins. TGF- β 1, TIMP-1 and MMP-9 have been reported to be significantly elevated in hepatocytes, and the extent of fibrosis is correlated with the magnitude of these increases.^{19,20}

However, insufficient information exists on the tolerance of RT in cirrhotic liver, even though RT is one of the treatments for HCC. Thus, it is necessary to have a good model and parameters that can be used to test treatment regimens.¹⁵ Specifically, this requires that new technologies, including proteomic analysis and gene expression profiling, be used to identify diagnostic markers and therapeutic and preventive targets.^{1,3}

In this study, we first made an animal model of the effects of radiation in rats with TAA-induced liver cirrhosis. After the length of time until development of liver cirrhosis was determined, another set of experimental animals was irradiated to assess hepatic injury in this TAA-induced liver cirrhosis model. Second, to examine the influence of radiation in liver cirrhosis, we identified proteins commonly expressed in liver tissue and serum following radiation exposure in TAA-induced liver cirrhosis using a proteomic analysis.

II. MATERIALS AND METHODS

1. Animals

Male Wistar rats weighing 200 ± 25 g were used. They were supplied by the Division of Laboratory Animal Medicine, College of Medicine, Yonsei University. Animals were cared in a specific pathogen-free (SPF) barrier area at the Division of Laboratory Animal Medicine, College of Medicine, Yonsei University. The temperature (22°C) and humidity (55%) were controlled constantly. Water (RO water) and food (PMI) were supplied *ad libitum*. The care and use of laboratory animals in these experiments were based on the Guidelines and Regulations for the Use and Care of Animals at Yonsei University.

2. Induction of liver cirrhosis

Rats were treated with thioacetamide (TAA; Sigma, St. Louis, MO, USA), which was dissolved in the rats' drinking water at a concentration of 0.3 g/L. The rats were given TAA in their water for 9 weeks. Also, liver cirrhosis was induced by intraperitoneal (i.p.) administration of TAA at a dose of 300 mg/kg twice a week for 16 weeks. The animals were killed after treatment, and the extent of liver cirrhosis was assessed by histological examination.

3. Experimental groups

For the analysis of hepatic injury from radiation, two experimental groups were established: TAA-alone and TAA-plus-radiation groups, with three rats in each group. The cirrhotic rats were treated with partial liver radiation. For radiation, the rats underwent a simulation, a process to determine the determining radiation field, under intramuscular (i.m.) anesthesia, with mixture of ketamine and xylazine. The partial liver, which was estimated as one-third of the whole liver, was treated with a single dose of 10 Gy using a linear accelerator (Varian Co., Milpitas, CA, USA). Then the rats were closely observed for 3 weeks after the radiation treatment.

4. Histological analysis

(1) Picro-Sirius red staining

The liver was sampled and fixed in 10% neutral-buffered formalin. The tissues were embedded in paraffin blocks and 4- μm sections were then cut and stained. The tissue sections were deparaffinized in xylene (3 \times 20 min) and rehydrated through a series of graded alcohols (100%, 95%, 90%, 80%, 70%) to diluted water. The deparaffinized sections were washed three times with PBS, and then soaked in 0.1% picro-sirius red solution for 45 min. After washing twice with 100% ethanol, sections were dipped in xylene.

For the quantitative analysis of liver fibrosis, the liver fibrosis area with picro-sirius red staining was quantified using a microscope (Olympus, Tokyo,

Japan) equipped with a CCD camera. Briefly, the red area, considered fibrotic, was assessed by computer-assisted image analysis using the Meta-Morph software (Universal Imaging Corporation, Downingtown, PA, USA) at a magnification of x40. The mean value from two randomly selected areas per sample was used as the percentage area of fibrosis.

(2) Immunohistochemical staining

Immunohistochemical staining was performed with 4- μm , formalin-fixed, paraffin-embedded tissue samples. After incubating the slide sections on a silane-coated slide overnight at 37°C, tissue sections were deparaffinized in xylene (3 \times 10 min) and rehydrated through a series of graded alcohols (100%, 95%, 90%, 80%, 70%) to diluted water. The deparaffinized sections were then heated and boiled (2 \times 10 min) by microwaving in 0.01 M citrate buffer (pH 6.0) to retrieve the antigens.

The antibody used was a mouse monoclonal antibody against proliferating cell nuclear antigen (PCNA; PC10; Dako A/S, Glostrup, Denmark) at 4°C for overnight. Antibody was used at the dilution recommended by the manufacturer. After washing three times with PBS, sections were incubated with a biotinylated linker (LSAB2; Dako A/S, Glostrup, Denmark) for 20 min. They were then washed three times with PBS, treated with streptavidin-HRP (LSAB2; Dako A/S, Glostrup, Denmark) for 20 min, and washed again with PBS three times. The peroxidase binding sites were detected by staining with diaminobenzidine (DAB; Dako A/S, Glostrup, Denmark), and the sections were finally counterstained with Mayer's hematoxylin and observed under a light microscope.

Quantitative analysis of immunohistochemical staining for PCNA at a

magnification of x400 was determined. The PCNA index was determined by counting the number of positive cells among at least 1000 cells, and was indicated as percentage.

5. Biochemical parameters

Measurement of albumin, total bilirubin, aspartate aminotransferase (AST), alanine aminotransferase (ALT) and alkaline phosphatase (ALP) was conducted by Seoul Clinical Laboratories using standard clinical methods.

6. Proteomic analysis

(1) Two-dimensional electrophoresis (2-DE)

A proteomic analysis was conducted in liver tissue and serum. The proteins from frozen liver tissue and serum were extracted in lysis buffer (7 M urea, 2 M thiourea, 4.5% CHAPS, 40 mM Tris, 100 mM dithiothreitol (DTT), 0.002% bromophenol blue) for 1 h at 4°C. Proteins (500 µg) were precipitated with three to five times with acetone for a further more 2 h at -20°C and then centrifuged (20 min, 14,000 rpm). After the supernatants were removed, the pellets were air-dried for 30 min. Lysis buffer (125 µl) supplemented with 0.5% carrier ampholyte (Bio-rad, Hercules, CA, USA) was then added. Samples were incubated

overnight at 4°C. After samples had spread immobilized pH gradient (IPG) strips (pH 3-10 NL; nonlinear, 17-cm long; Bio-rad, Hercules, CA, USA) were applied to the samples and incubated for 1 h at room temperature. Mineral oil (1 mL) was added to the IPG strips, and they were rehydrated for more than 16 h to passive. Isoelectric focusing (IEF) was initiated at 100 V for 2 h and then gradually increased. After IEF, the IPG strips were equilibrated with 10 mL buffer (6 M urea, 50 mM Tris-HCl (pH 8.8), 20% glycerol, 2% SDS), supplemented with 0.1 g DTT, and then 10 mL buffer supplemented with 0.125 g iodoacetamide for 15 min in a shaker. After gently washing with running buffer, SDS PAGE was performed on a 9-18% gradient gel. The gel was fixed and stained with Coomassie brilliant blue G-250.

(2) In gel digestion

Gel spots were randomly selected and acquired with end-cut yellow tips. Spots were washed three times with deionized water (dH₂O), and after incubation with 100 mM ammonium bicarbonate for 20 min, they were gently vortexed in 100% acetonitrile (SIGMA, Saint Louis, MS, USA). This process was repeated. Gel spots were air-dried for 10 min and incubated with 100 μ l of 100 mM ammonium bicarbonate, supplemented with 1 μ l of 1 M DTT, for 30 min at 56°C. A solution (100 μ l) containing 10 mg iodoacetamide per 1 mL and 100 mM ammonium bicarbonate was added to the gel spots and then incubated for 30 min at room temperature, protected from light. The gel spots were vortexed in 30 μ l 100% acetonitrile for 3 min and then 50 μ l 100% acetonitrile. After air-drying for 10 min, gel spots were incubated with

10 $\mu\text{g}/\text{mL}$ trypsin (Promega, Madison, WI, USA) at 4°C for 30 min and then in 50 mM ammonium bicarbonate overnight at 37°C in a shaking incubator. They were then sonicated for 30 min, and the supernatants were removed and dried under vacuum.

(3) Quadrupole time of flight (Q-TOF) mass spectrometry (MS) and data processing

Nanoflow LC separation was carried out with a CapLC device from Waters (Milford, MA, USA). The analytical column (150 cm x 75 μm) was prepared. The tip at the end of the capillary tubing (75 μm I.D. x 360 μm O.D.) from Polymicro Technology LLC (Phoenix, AZ, USA) was pulled in a flame to a tip diameter of around 10 μm . Then, the pulled tip capillary with an end frit (~1 mm in length) was packed with a methanol slurry of 5- μm 100 Magic C₁₈AQ (Michrom BioResources Inc., Auburn, CA, USA) at a constant pressure (1000 psi). The analytical column was connected via a PEEK microcross, and a gold wire was used as an electrode to supply an electrospray ionization voltage of 2.3 kV. To separate the peptide mixtures extracted from the gel spots, a binary gradient RPLC separation was carried out by varying the mobile phase composition of (A) 2% acetonitrile (ACN) in water and (B) 98% ACN. Both mobile phases contained 0.1% (v/v) formic acid. The gradient began with an increase to 5% B (from 2% B at default) over 4 min and ramped to 20% for 60 min, and to 32% B for 20 min. Then, it was raised to 80% B for 2 min, maintained for 20 min, reduced to 2% B over 3 min, and maintained for at least 20 min for column reconditioning. The flow rate during the gradient separation was kept at 200 nL/min and the eluted peptides were electrosprayed directly into the mass spectrometer.

A Q-TOF mass spectrometer model (Waters; Milford, MA, USA) was used. Peptide ions were detected in a data-dependent analysis mode. The acquisition method involved one MS precursor scan from 300 to 1800 amu, followed by three data dependent MS/MS scans (35% normalized collision energy).

The acquired MS-MS spectra were analyzed using the Mascot Search program and then compared with the Swiss-Prot human protein database. The mass tolerance between the measured monoisotopic mass and the calculated mass was 1.0 u for the molar mass of a precursor peptide and 1.0 u for the mass of peptide fragment ions. Only those peptides yielding a Mascot score above 40 were selected, indicating identification at the 95% confidence level for this search.

7. Western blot analysis

Proteins identified were validated by Western blotting. Liver tissues and serum were collected from TAA-treated rats and irradiated rats with TAA-induced liver cirrhosis. Small pieces of liver tissue were washed three times in ice-cold phosphate-buffered saline (PBS), and lysed in a cold buffer containing 100 mM HEPES, 200 mM NaCl, 20% glycerol, 2% NP40, 2 mM EDTA, 40 mM β -glyceraldehyde-phosphate, 2 mM sodium fluoride, 1 mM DTT, 1 mM sodium orthovanadate, 0.2 mM phenylmethyl sulfonyl fluoride, 5 μ g/mL leupeptin, and 2 μ g/mL aprotinin for 1 h. The samples were centrifuged (4°C, 20 min) and supernatants were transferred into new tubes. The lysates were then denatured at 100°C for 5 min in the presence of 5% mercaptoethanol and loaded onto polyacrylamide gels. Proteins applied to each lane of the polyacrylamide gel were adjusted to equal concentrations using a Bio-Rad protein assay (Bio-Rad,

Hercules, CA, USA). Proteins were fractionated using SDS-PAGE and transferred onto a nitrocellulose membrane (Milipore Corporation, Bedford, MA, USA) in a transfer buffer consisting of 48 mM Tris base, 20% methanol, 0.04% SDS, and 30 mM glycine. After gentle washing in Tris-buffered saline (TBS), the membrane was blocked in 3% BSA for 1 h at room temperature. Rabbit anti-HPA 2/3 (H-100) (Santa Cruz Biotechnology, Santa Cruz, CA, USA) and rabbit anti-Met (C-28) (Santa Cruz Biotechnology, Santa Cruz, CA, USA) were diluted both 1:200 in 0.5% skim milk, and were then incubated overnight at 4°C. The membrane was washed three times using TBS with 0.1% Tween 20 (TBST) for 10 min and incubated with horseradish peroxidase (HRP)-conjugated secondary antibodies for 1 h at room temperature. It was washed three times with TBST for 10 min. Detectable proteins were quantitated using densitometry (Amersham Pharmacia Biotech, Piscataway, NJ, USA) after chemiluminescent detection (Fuji Photo film, Tokyo, Japan) and the ECL Western blotting detection system (Amersham Pharmacia Biotech, Piscataway, NJ, USA).

8. Statistical analysis

The results are expressed as the mean \pm SE. For comparison of means, a *t*-test was used. All tests were two-sided, and a *p*-value less than 0.05 was deemed to indicate statistical significance.

III. RESULTS

1. Optical examination of TAA-induced liver cirrhosis in rats

Male Wistar rats were treated with 0.3 g/L TAA in their drinking water for 9 weeks. Another set of rats was partially irradiated. Optical examination of rat livers showed little difference from the initial cirrhotic features after 9 weeks of treatment with TAA. After irradiation, a gross photograph of the liver with a little nodular surface was taken (Fig. 1).

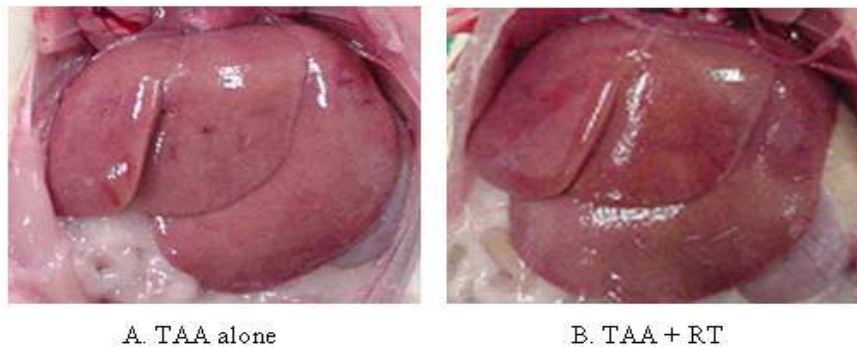


Figure 1. Photographs of rat liver with TAA-induced cirrhosis (A) and TAA plus partial radiation treatment (B). Optical examination showed slight differences between the TAA-alone (A) and TAA-plus-radiation groups (B).

2. Measurement of liver weight

Body and liver weights were measured after the treatment (Table 1). Although the liver weight of the TAA-plus-radiation group showed a mild increase compared to the TAA-alone group, the ratio of liver/body weight showed a slight, but statistically nonsignificant, increase ($p > 0.05$).

Table 1. Comparison of liver/body weight ratio between TAA-alone group and TAA-plus-radiation group

	TAA alone	TAA + radiation	p value*
Body weight (g)	386 \pm 10.2	378 \pm 8.51	0.043
Liver weight (g)	17.2 \pm 0.92	20 \pm 1.32	0.115
The ratio of liver/body weight	0.04 \pm 0.002	0.05 \pm 0.003	0.100

* t -test.

3. Histological assay and measurement of fibrotic area

At 3 weeks following TAA administration for 9 weeks, the livers were examined. Liver sections of TAA-treated rats and irradiated rats with TAA-induced liver cirrhosis were stained with Masson's trichrome and Picro-sirius red. The histological feature showed that liver of normal control had no specific alterations. However, the degree of liver fibrosis in TAA-treated rats had increased. At 9 weeks after TAA administration, liver fibrosis was observed. Masson's trichrome and picro-sirius red stain specifically for collagen I/III-containing fibers were applied. The staining showed a normal distribution of fibrous tissues around vascular structures in the normal control group, while significant fibrosis was seen in the TAA-alone group. After irradiation, more fibrosis was seen than in the TAA-alone group (Fig. 2).

The percent area of liver fibrosis was calculated using picro-sirius red staining as described in the Materials and Methods. Briefly, the red area, considered fibrotic, was assessed by computer-assisted image analysis using the Meta-Morph software at a magnification of x40. The percent area of liver fibrosis was approximately 23% in the TAA-alone group (Fig. 3); in the TAA-plus-radiation group, it was 32%, corresponding to mildly enhanced liver fibrosis (Fig. 3).

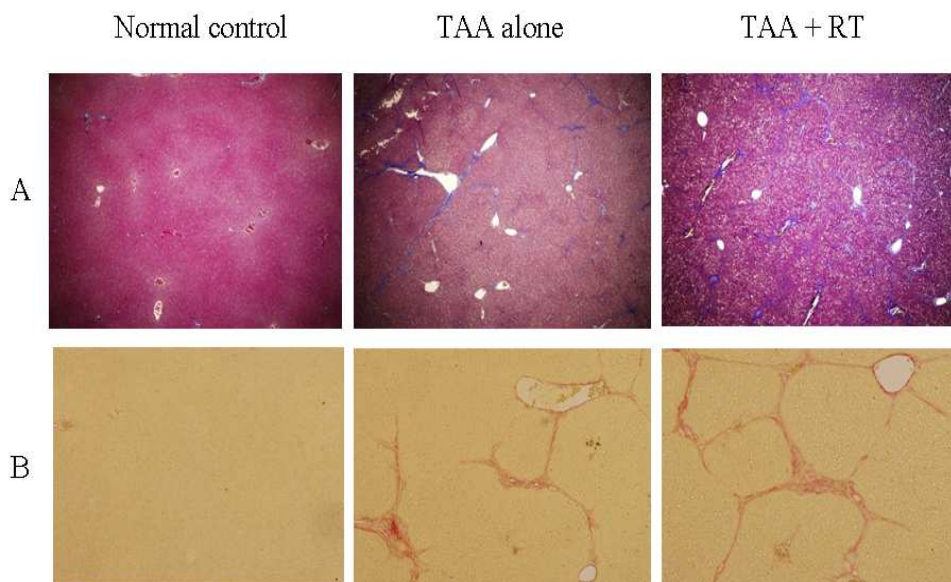


Figure 2. Histological analysis of liver sections using (A) Masson's trichrome and (B) picro-sirius red stain (original magnification, x40).

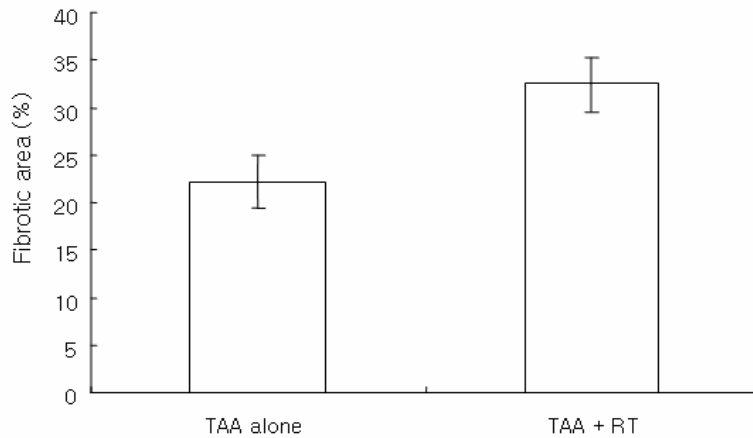


Figure 3. Quantitative analysis of liver fibrosis assessed by computer-assisted image analysis in the TAA-alone and TAA-plus-radiation groups. Percent area of liver fibrosis was calculated using picro-sirius red staining, as described in the Materials and Methods. Percent area of liver fibrosis increased almost 1.4-fold following radiation exposure.

4. Assessment of biochemical parameters in experimental groups

Liver injury is generally assessed using histological analysis and biochemical parameters in serum. Thus, various parameters of liver injury including albumin, total bilirubin, AST, ALT, and ALP were analyzed in serum by intraperitoneal administration of TAA in TAA-alone and TAA-plus-radiation groups.

Albumin, ALT and ALP decreased in the TAA-plus-radiation group compared to the TAA-alone group. The difference in albumin was statistically significant ($p < 0.05$); however, the difference in ALT and ALP was not ($p > 0.05$). The value of total bilirubin increased in the TAA-plus-radiation group ($p < 0.05$). No significant difference in AST was noted between the groups ($p > 0.05$).

Table 2. Biochemical parameters in serum by intraperitoneal administration of TAA

	TAA alone	TAA + radiation	p value*
Albumin (g/dL)	3.13 ± 0.17	2.8 ± 0.13	0.015 †
Total bilirubin (mg/dL)	0.02 ± 0.01	0.05 ± 0.00	0.030 †
AST (U/L)	117.33 ± 21.22	113.5 ± 12.91	0.890
ALT (U/L)	87.33 ± 12.16	60.25 ± 9.62	0.256
ALP (U/L)	289 ± 26.01	206 ± 33.51	0.243

* t -test.

† $p < 0.05$, the value was statistically significant.

5. Proteomic analysis and validation

In the proteomic analysis of liver tissue and serum, the expression pattern of proteins differed significantly between the TAA-alone and TAA-plus-radiation groups (Fig. 4). In 2-DE, protein spots were separated: about 800 in serum and about 1700 in liver tissue. Screening of serum showed that 6 protein spots were up-regulated and 9 protein spots were down-regulated in the TAA-plus-radiation group compared to the TAA-alone group by a factor of at least two in each case. Additionally, screening of liver tissue showed that 22 protein spots were up-regulated and 20 protein spots were down-regulated in the TAA-plus-radiation group compared to the TAA-alone group by a factor of at least two in each case. These protein spots were processed using in gel enzymatic digestion and Q-TOF, allowing their identification.

The identified proteins had functions in the immune response, signal transduction, apoptosis, proliferation/differentiation, and reactive oxygen species metabolism. Proteins commonly seen in both liver tissue and serum following radiation included the heparanase precursor and hepatocyte growth factor receptor. Expression of the heparanase precursor increased more than twofold in the TAA-plus-radiation group compared to the TAA-alone group, while expression of the hepatocyte growth factor receptor decreased more than twofold in the TAA-plus-radiation group (Table 3).

These proteins were validated using Western blotting. The expression of the heparanase precursor increased in the TAA-plus-radiation group compared to the TAA-alone group, while the expression of hepatocyte growth factor receptor decreased in the TAA-plus-radiation group (Fig. 5).

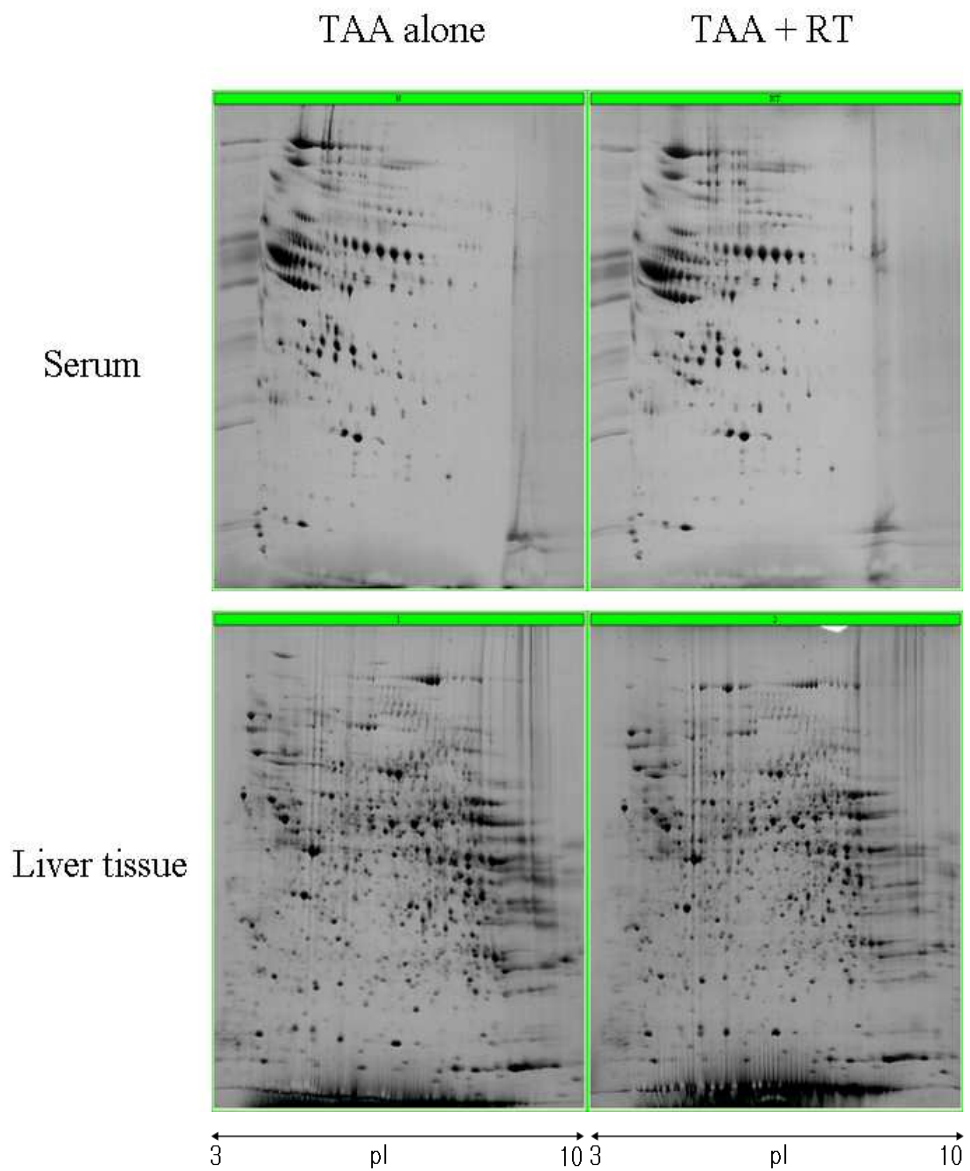


Figure 4. Differential expression of proteins between the TAA-alone and TAA-plus-radiation groups in liver tissue. Serum proteins also showed differential expression.

Table 3. Proteins that were altered by radiation

Pattern:		
TAA alone→		
TAA + RT	Proteins in serum	Proteins in liver tissue
Twofold increase	<ul style="list-style-type: none"> • Ceruloplasmin precursor (Ferroxidase) • Collagen alpha-1 (XI) chain precursor • Heparanase precursor • Apolipoprotein E precursor • Proteasome subunit alpha type 4 	<ul style="list-style-type: none"> • Tumor necrosis factor, alpha-induced protein 3 • Thioredoxin reductase 2, mitochondrial precursor • Catenin alpha-1 • Stress-70 protein, mitochondrial precursor • Cytochrome P450 2C12 • Heparanase precursor • Interleukin-4 receptor alpha chain precursor • Caspase recruitment domain-containing protein 15 • Tumor necrosis factor receptor superfamily member 6 precursor • Transforming growth factor beta-1 precursor
Twofold decrease	<ul style="list-style-type: none"> • T-cell surface glycoprotein CD5 precursor • Activation signal cointegrator 1 complex subunit 1 • Retinoblastoma-like protein 1 • Hepatocyte growth factor receptor precursor • Ras GTPase-activating protein 2 • Plasminogen precursor 	<ul style="list-style-type: none"> • Adenomatous polyposis coli protein • Cytochrome P450 2B11 • Hepatocyte growth factor receptor precursor • Coagulation factor 7 precursor • Metallothionein-1F • Transformation/transcription domain associated protein • Ubiquitin-protein ligase E3 Mdm2 • Platelet endothelial cell adhesion molecule precursor • Collagen alpha-1(III) chain precursor • Metallothionein-1A

* Increase and decrease: approximate twofold different change of protein.

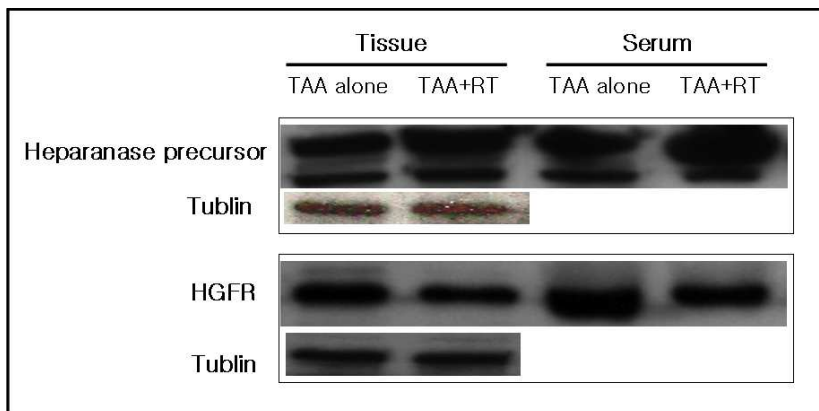


Figure 5. Common proteins in both liver tissue and serum following radiation included the heparanase precursor and hepatocyte growth factor receptor; these were validated using Western blotting.

6. Immunohistochemical staining for PCNA and hematoxylin and eosin (H&E) staining for apoptosis

To determine if irradiation was associated with the decreased hepatocyte growth factor receptor, paraffin-embedded liver tissues were immunohistochemically stained with an anti-PCNA antibody (Fig. 6). PCNA was expressed primarily in the nuclei of hepatocytes. When TAA-induced cirrhotic rats were radiation-treated, the expression of PCNA decreased compared to the TAA-alone group. The staining of PCNA showed a similar pattern to that of the hepatocyte growth factor receptor.

Liver injury was evaluated in sections embedded in paraffin and stained with H&E (Fig. 7). Radiation treatment of cirrhotic liver induced extensive micronodular and macronodular cirrhosis, with signs of cell damage in hepatocytes. In addition, nuclei in hepatocytes showed that apoptosis was induced in irradiated liver tissue.

The PCNA and apoptotic indices were determined by counting the number of positive cells among at least 1000 cells, and are indicated as a percentage (Fig. 8). The percentage of PCNA-positive cells decreased markedly, about 1.8-fold, in the TAA-plus-radiation group compared to the TAA-alone group. The percentage of apoptotic cells significantly increased, by almost 5-fold following radiation treatment. These data suggest that radiation enhanced the hepatic injury in TAA-induced liver cirrhosis.

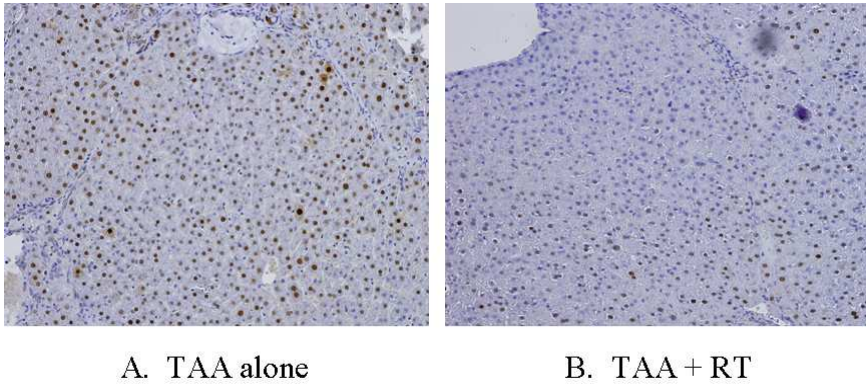


Figure 6. Immunohistochemical staining for PCNA in liver sections. PCNA-positive cells decreased markedly in the TAA-plus-radiation group (B) compared to the TAA-alone group (A) (original magnification, x200).

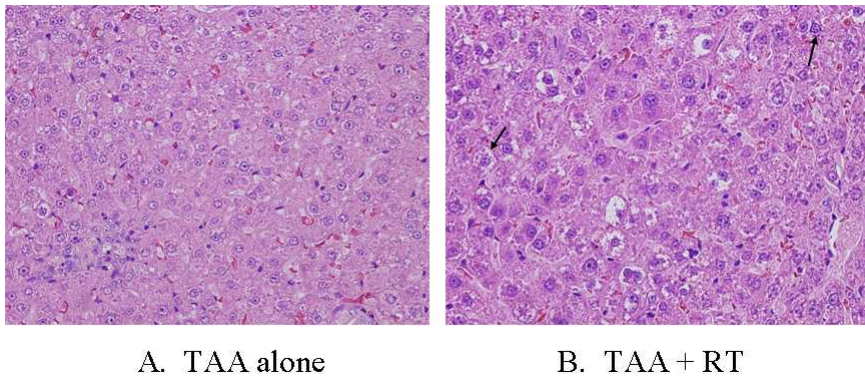


Figure 7. Hematoxylin and eosin stained liver sections after TAA treatment (A) and TAA-plus-radiation (B) showed increased apoptotic cells (arrows), identified by histological criteria (original magnification, x400).

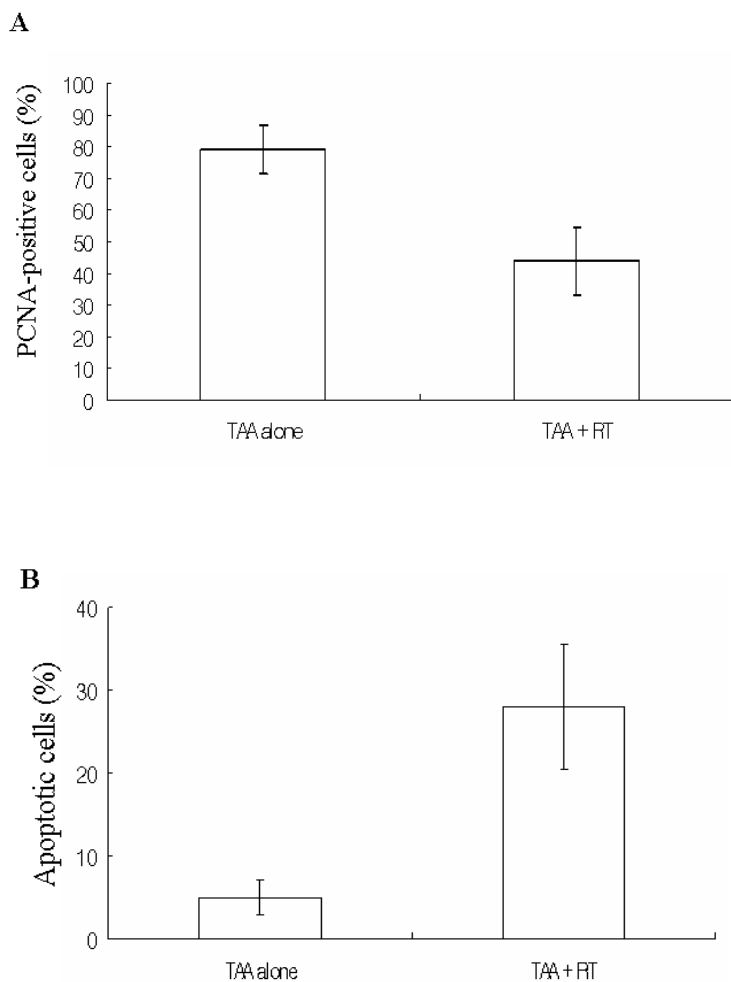


Figure 8. Quantitative analysis of immunohistochemical staining for PCNA (A) and hematoxylin and eosin staining (B) at a magnification of x400. The percentage of PCNA-positive cells decreased markedly, about 1.8-fold, in TAA-plus-radiation group compared to the TAA-alone group (A). The percentage of apoptotic cells increased almost 5-fold following radiation treatment (B).

IV. DISCUSSION

In the present study, liver cirrhosis was established by TAA administration, and proteins were identified commonly that were expressed both in liver tissue and serum following radiation using a proteomic analysis. Histological analysis of liver tissues and biochemical parameters of serum revealed that the degree of hepatic injury was increased by irradiation in the TAA-induced rat cirrhotic model.

Proteomic analysis of liver tissue and serum showed that the expression pattern of proteins following radiation in liver cirrhosis differed significantly. Proteins commonly seen in both liver tissue and serum following radiation included the heparanase precursor and hepatocyte growth factor receptor.

Expression of the heparanase precursor increased in both liver tissue and serum following radiation in TAA-induced liver cirrhosis. Heparanase activity has been reported to be correlated with the extravasation and progression of cancer cells in an animal model and human cancer.^{21,22} In addition, heparanase contributes to metastasis and angiogenesis in cancer cells.²³⁻²⁹ A characteristic of cancer cells is invasion into the surrounding matrix.³⁰ To degrade the extracellular matrix, cells express heparanase, an endoglycosidase, which is a cell surface- and extracellular matrix-degrading enzyme.³¹⁻³³ It cleaves heparan sulfate proteoglycans (HSPGs) into heparan sulfate side chains and core proteoglycans.^{23,34} However, little is known about the regulation of heparanase expression.³¹

To investigate hepatic injury following radiation in liver cirrhosis, liver tissue was assessed after H&E staining. Nuclei in hepatocytes showed that apoptosis was induced following radiation. Thus, apoptotic hepatocytes, identified by histological criteria, markedly increased following radiation in liver cirrhosis. These data suggest that radiation enhanced the hepatic injury in TAA-induced liver cirrhosis.

In the proteomics and Western blot analyses, the expression of hepatocyte growth factor receptor (HGFR, c-MET) significantly decreased in the radiation-treated animals. Additionally, HGFR decreased in both liver tissue and serum.

Hepatocyte growth factor (HGF), a ligand for the HGFR proto-oncogene product, is the most potent stimulator of hepatocyte proliferation. HGF exerts multiple biological properties in the liver, including antifibrotic and cytoprotective activities.^{35,36} It is also a major mitogen in early liver regeneration after liver injury. HGFR is a receptor for HGF and scatter factor, and has tyrosine kinase activity. HGF and its specific receptor, HGFR, play a pivotal role in hepatocyte proliferation.³⁶⁻³⁹

These results indicate that the proliferating capacity of hepatocytes following radiation in cirrhotic livers may be induced by decreased HGFR. Accordingly, the proliferating capacity of hepatocytes is severely impaired and extracellular matrix components are deposited to retrieve space lost by the destruction of hepatocytes, resulting in the progression of liver cirrhosis.^{35,40,41}

An important cause of liver cirrhosis appears to be the impaired proliferating capacity of hepatocytes caused by continuous hepatic damage.⁴² To estimate the proliferating capacity of hepatocytes, liver tissue was stained immunohistochemically for PCNA. The number of

PCNA-positive cells decreased markedly following radiation in TAA-induced cirrhotic liver. The decreased expression of PCNA following radiation was similar to that of HGFR.

The expression of HGFR and PCNA both decreased following radiation, suggesting that radiation reduced proliferating capacity of hepatocytes in TAA-induced liver cirrhosis.

Few specific biomarkers of hepatic injury following radiation in liver cirrhosis, can be used for diagnostic criteria. Moreover, single measurements of biochemical markers in serum, plasma, or even urine, are presently not sufficiently valid to replace liver biopsies. Thus, it would be helpful necessary biological indicators that provide information about hepatic injury caused by radiation in liver cirrhosis.

The present study identified protein biomarkers that could be detected commonly in serum and liver tissue following radiation in a rat cirrhosis model. Proteins are suitable biomarkers because changes in protein levels are often more pronounced than changes in mRNA expression. These proteins may be useful markers for predicting and monitoring of radiation-induced hepatic injury.⁴³⁻⁴⁵

More detailed experiments are required to establishment these proteins as biomarkers for clinical diagnosis and therapy.

V. CONCLUSION

In conclusion, radiation induced hepatic fibrosis and apoptosis in TAA-induced liver cirrhosis. Proteomic analysis identified proteins with various functions that were altered by the radiation. Specifically, the heparanase precursor increased and the hepatocyte growth factor receptor decreased both in liver tissue and serum, suggesting that radiation worsened the liver cirrhosis. The results of this study show that radiation should be applied with extreme caution in patients with cirrhosis. Hopefully, these proteins may be useful in detecting and monitoring radiation-induced hepatic injury and ultimately in improving therapeutic outcome in these patients with cirrhosis.

REFERENCES

1. Blum H. Hepatocellular carcinoma: Therapy and prevention. *World J Gastroenterology* 2005;11;7391-7400.
2. Okuda K. Hepatocellular carcinoma. *J Hepatol* 2000;32;225-237.
3. Bruix J, Llovet JM. Prognostic prediction and treatment strategy in hepatocellular carcinoma. *Hepatology* 2002;35;519-524.
4. Kim TH, Kim DY, Park JW, Kim YI, Kim SH, Park HS, et al. Three-dimensional conformal radiotherapy of unresectable hepatocellular carcinoma patients for whom transcatheter arterial chemoembolization was ineffective or unsuitable. *American Journal of Clinical Oncology* 2006;29;568-575.
5. Park W, Lim DH, Paik SW, Koh KC, Choi MS, Park CK, et al. Local radiotherapy for patients with unresectable hepatocellular carcinoma. *Int. J. Radiation Oncology Biol. Phys.* 2005;61;1143-1150.
6. Seong J, Keum KC, Han KH, Lee DY, Lee JT, Chon CY, et al. Combine transcatheter arterial chemoembolization and local radiotherapy of unresectable hepatocellular carcinoma. *Int. J. Radiation Oncology Biol. Phys.* 1999;43;393-397.
7. Dusheiko GM, Hobbs KE, Dick R, Burroughs AK. Treatment of small hepatocellular carcinoma. *Lancet* 1992;340;285-288.
8. Park HC, Seong J, Han KH, Chon CY, Moon YM, Suh CO. Dose-response relationship in local radiotherapy for hepatocellular carcinoma. *Int. J. Radiation Oncology Biol. Phys.* 2002;54;150-155.
9. Cheng JCH, Wu JK, Lee PCT, Liu HS, Jian JJM, Lin YM, et al. Biologic susceptibility of hepatocellular carcinoma patients treated with

- radiotherapy to radiation-induced liver disease. *Int. J. Radiation Oncology Biol. Phys.* 2004;60:1502-1509.
10. Ohto M, Yoshikawa M, Saisho H, et al. Non surgical treatment of hepatocellular carcinoma in cirrhotic patients. *World J Surg* 1995;19:42-1946
 11. Tsuzuki T, Sugioka A, Ueda M. Hepatic resection for hepatocellular carcinoma. *Surgery* 1990;107:511-520.
 12. Seong J, Park HC, Han KH, Chon CY, Chu SS, Kim GE, et al. Clinical results of 3-dimensional conformal radiotherapy combined with transarterial chemoembolization for hepatocellular carcinoma in the cirrhotic patients. *Hepatology Research* 2003;27:30-35.
 13. Liang SX, Zhu XD, Xu ZY, Zhu J, Zhao JD, Lu HJ. Radiation-induced liver disease in three-dimensional conformal radiation therapy for primary liver carcinoma: The risk factors and hepatic radiation tolerance. *Int. J. Radiation Oncology Biol. Phys.* 2006;65:426-434.
 14. Ingold JA, Reed GB, Kaplan HS, et al. Radiation hepatitis. *Am J Roentgenol* 1965;93:200-208.
 15. Seong J, Han KH, Park YN, Nam SH, Kim SH, Keum WS. Lethal hepatic injury by combined treatment of radiation plus chemotherapy in rats with thioacetamide-induced liver cirrhosis. *Int. J. Radiation Oncology Biol. Phys.* 2003;57:282-288.
 16. Livraghi T, Bolondi L, Buscarini L, et al. No treatment, resection and ethanol injection in hepatocellular carcinoma: A retrospective analysis of survival in 391 patients with cirrhosis. Italian Cooperative HCC Study Group. *J Hepatol* 1995;22:522-526.
 17. Castells A, Bruix J, Bru C, et al. Treatment of small hepatocellular carcinoma in cirrhotic patients: A cohort study comparing surgical resection and percutaneous ethanol injection. *Hepatology* 1993;18:1121-1126.

18. Tanaka K, Nakamura S, Numata K, et al. The long term efficacy of combined transcatheter arterial embolization and percutaneous ethanol injection in the treatment of patients with large hepatocellular carcinoma and cirrhosis. *Cancer* 1998;82:78-85.
19. An JH, Seong J, Oh HJ, Kim WW, Han KH, Paik YH. Protein expression profiles in a rat cirrhotic model induced by thioacetamide. *The Korean Journal of Hepatology* 2006;12:93-102.
20. Seong J, Kim SH, Chung EJ, Lee WJ, Suh CO. Early alteration in TGF- β mRNA expression in irradiated rat liver. *Int. J. Radiation Oncology Biol. Phys.* 2000;46:639-643.
21. Ikeguchi M, Hirooka Y, Kaibara N. Heparanase gene expression and its correlation with spontaneous apoptosis in hepatocytes of cirrhotic liver and carcinoma. *European Journal of Cancer* 2003;39:86-90.
22. Hulett MD, Freeman C, Hamdorf BJ, Baker RT, Harris MJ, Parish CR. Cloning of mammalian heparanase, an important enzyme in tumor invasion and metastasis. *Nature Med* 1999;5:803-809.
23. Parish CR, Freeman C, Hulett MD. Heparanase: a key enzyme involved in cell invasion. *Biochim Biophys Acta* 2001;1471:99-108.
24. Vlodavsky I, Friedmann Y, Elkin M, et al. Mammalian heparanase: gene cloning, expression and function in tumor progression and metastasis. *Nature Med* 1999;5:793-802.
25. Xiao Y, Kleeff J, Shi X, Buchler MW, Friess H. Heparanase expression in hepatocellular carcinoma and the cirrhotic liver. *Hepatol Res* 2003;26:192-198.
26. Gohji K, Okamoto M, Kitazawa S, et al. Heparanase protein and gene expression in bladder cancer. *J Urol* 2001;166:1286-1290.
27. Elkin M, Ilan N, et al. Heparanase as mediator of angiogenesis: mode of action. *FASEB J* 2001;15:1661-1663.

28. Nakajima M, Irimura T, Nicolson GL. Heparanase and tumor metastasis. *J Cell Biochem* 1988;36:157-167.
29. Koliopoulos A, Friess H, Kleeff J, et al. Heparanase expression in primary and metastatic pancreatic cancer. *Cancer Res* 2001;61:4655-4659.
30. Nakajima M, Irimura T, Di Ferrante N, Nicolson GL. Metastatic melanoma cell heparanase. Characterization of heparansulfate degradation fragments produced by B16 melanoma endoglucuronidase. *J Biol Chem* 1982;259:2283-2290.
31. Goldshmidt O, Yeikilis R, Mawasi N, Paizi M, Gan N, Ilan N, Pappo O, et al. Heparanase expression during normal liver development and following partial hepatectomy. *J Pathol* 2004;203:594-602.
32. Iozzo RV. Heparanase sulfate proteoglycans: intricate molecules with intriguing functions. *J Clin Invest* 2001;108:165-167.
33. Vlodavsky I, Miao HQ, Medalion B, Danagher P, Ron D. Involvement of heparan sulfate and related molecules in sequestration and growth promoting activity of fibroblast growth factor. *Cancer Metastasis Rev* 1996;15:177-186.
34. Vlodavsky I, Friedmann Y. Molecular properties and involvement of heparanase in cancer metastasis and angiogenesis. *J Clin Invest* 2001;108:341-347.
35. Corpechot C, Barbu V, Wendum D, Chignard N, Housset C, Poupon R, et al. Hepatocyte growth factor and c-MET inhibition by hepatic cell hypoxia. *American Journal of Pathology* 2002;160:613-620.
36. Gherardi E, Sandin S, Petoukhov MV, Finch J, Youles ME, Ofverstedt LG, et al. Structural basis of hepatocyte growth factor/scatter factor and MET signalling. *PNAS* 2006;103:4046-4051.
37. Lindroos PM, Zarnegar R, Michalopoulos GK. Hepatocyte growth

- factor (hepatopoietin A) rapidly increases in plasma before DNA synthesis and liver regeneration stimulated by partial hepatectomy and carbon tetrachloride administration. *Hepatology* 1991;13;743-750.
38. Shiota G, Wang TC, Nakamura T, Schmidt EV. Hepatocyte growth factor in transgenic mice: effects on hepatocyte growth, liver regeneration and gene expression. *Hepatology* 1994;19;962-972.
 39. Kaibori M, Kwon AH, Nakagawa M, Wei T, et al. Stimulation of liver regeneration and function after partial hepatectomy in cirrhotic rats by continuous infusion of recombinant human hepatocyte growth factor. *J Hepatol* 1997;27;381-390.
 40. Qian LW, Mizumoto K, Inadome N, Nagai E, Sato N, et al. Radiation stimulates HGF receptor/c-Met expression that leads to amplifying cellular response to HGF stimulation via upregulated receptor tyrosine phosphorylation and MAP kinase activity in pancreatic cancer cells. *Int. J. Cancer* 2003;104;542-549.
 41. Lai B, Xia S, Abounader R, Laterra J. Targeting the c-MET pathway potentiates glioblastoma responses to r-radiation. *Clin Cancer Res* 2005;11(12);4479-4486.
 42. Inoue H, Yokoyama F, Kita Y, Yoshiji H, Tsujimoto T, Deguchi A, et al. Relationship between the proliferative capability of hepatocytes and the intrahepatic expression of hepatocyte growth factor and c-Met in the course of cirrhosis development in rats. *Int J Mol Med*. 2006;17(5);857-864.
 43. Lee HJ, Lee M, Kang CM, Jeoung D, Bae S, Cho CK, et al. Identification of possible candidate biomarkers for local or whole body radiation exposure in C57BL/6 mice. *Int. J. Radiation Oncology Biol. Phys.* 2007;69;1272-1281.
 44. Park WY, Hwang CI, Im CN, et al. Identification of radiation-specific

- responses from gene expression profile. *Oncogene* 2002;21;8521-8528.
45. Snyser AR, Morgan WF. Gene expression profiling after irradiation: Clues to understanding acute and persistent responses? *Cancer Metast* 2004;23;259-268.

ABSTRACT (IN KOREAN)

랫드 간경변 모델에서
방사선에 의한 간손상의 표적 단백질의 탐색

<지도교수 한 광 협>

연세대학교 대학원 의과학과

정 숙 인

간세포암은 전세계적으로, 특히 아시아에서 흔하게 발생하는 암 중의 하나로써, 병의 빠른 진행과 간경변증의 동반과 같은 문제로 인하여 예후가 좋지 않다. 방사선 치료는 간세포암을 위한 여러 치료 방법들 중의 하나로, 초기 간경변증을 동반한 간세포암에서 방사선 치료가 시행되고 있다. 그러나 간경변증을 동반한 간에 방사선 조사로 인하여 간 기능이 악화되는 기전에 대한 체계적인 연구가 미흡한 상황이다.

본 연구에서는 Thioacetamide (TAA)로 유도한 랫드 간경변 모델에 방사선을 조사하였을 때 간조직과 혈액에서 공통적으로 발현하는

단백질을 알아보고, 그 기능을 규명하고자 하였다.

웅성 Wistar 랫드에 0.3 g/L TAA를 음용수에 희석하여 9주 동안 복용시켜 간경변을 유발하였고, 간경변을 가진 랫드의 일부는 10 Gy의 방사선을 간의 우엽에만 부분 조사하였다. 랫드는 방사선 조사 후 3주까지 관찰하였고, 획득한 간 조직과 혈액은 프로테오믹스 기법을 이용하여 분석하고 확인하였다.

조직, 형태학적 분석을 통해 간경변증을 동반한 간에 방사선을 조사하면 간 섬유화가 증가됨을 볼 수 있었다. 간 조직과 혈액의 프로테오믹스 결과, 총 57개의 단백질이 방사선에 의해 발현의 차이를 보였다. 발현된 단백질은 기능별로 구별한 결과 면역반응, 신호변환, 세포사멸, 증식/분화, 대사에 관여하는 단백질로 나타났다. 방사선 조사 후, heparanase precursor는 증가하고 hepatocyte growth factor receptor는 감소하는 양상이 간 조직과 혈액에서 공통적으로 발현되었다. Proliferating cells nuclear antigen (PCNA)의 발현은 방사선 조사 후 감소하였으며, H&E 염색을 통해 관찰한 세포사멸은 방사선 조사 후에 증가하였다.

TAA로 유도한 랫드 간경변 모델에서 방사선 조사로 인해 간섬유화와 세포사멸이 증가함을 관찰하였고, 간조직과 혈액 내 단백질의 변화를 확인하였다. 방사선 조사 후에 간 조직과 혈액에서 공통적으로 heparanase precursor가 증가하고 hepatocyte growth factor receptor가 감소되었으며, 이 단백질이 아마도 향후 방사선 치료에 의한 간 손상을 인지하고 치료를 개선할 수 있는 방법 개발에 유용할 것으로 생각된다.

핵심되는 말 : 간경변증, 방사선, 프로테오믹스, 간 손상